IMPROVEMENT OF DRAINAGE OPERATIONAL SCHEME IN PUMPED FIELD LOWLAND

N. Cao Don[1], **H. Araki**[2], **H. Yamanishi**[2], **K. Koga**[3]

[1]Student, Institute of Lowland Technology, Saga University, Saga, Japan
[2]Prof., Institute of Lowland Technology, Saga University, Saga, Japan
[3]Prof., Dept. of Civil Engineering, Saga University, Saga, Japan

1. INTRODUCTION

Ha Nam area, located at about 20°36' North and 106°10' East, is the relatively flat and lowland area of the Red River, Vietnam, as shown in Fig. 1. The interior land is protected by banks and dykes system and bordered by four surrounding rivers, the Chau River and the Red River in the North, the Day River and the Dao River in the South. The total drainage area is 85,326 ha. The channel network systems with total length of 105 km serve many other canals and pumping stations. There are six large pumping stations with total pumping capacity of 220 m^3/s and the drainage coefficient q=2.89 l/s/ha.

During rainy season, frequent flooding by storm water is one of the most serious problems of this area, causing heavy effect on many economic activities. As the required drainage water levels in this area are lower than the water level of the bounded rivers, the excessive water cannot be drained out by gravity flow; therefore it must be pumped out. The drainage system should be operated appropriately taking account of tidal effect, rainfall intensity and combination of drainage facilities. Such proper operating systems have not been established yet in the region. In this study, mitigation scenarios are introduced to improve the drainage system by operating gates and pumps.

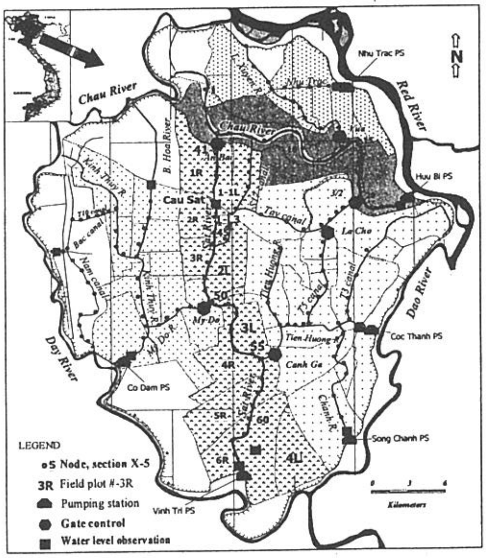

Fig. 1 Location map of the study area

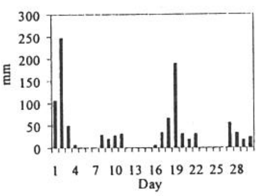

Fig. 2 Rainfall pattern, 28th Aug to 27th Sept, 1994

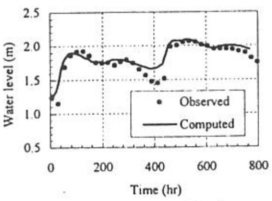

Fig. 3 Model calibration: Water level at Cau Sat

2. UNSTEADY FLOW MODEL

Flow in an open channel is governed by the equations of motion and conservation of mass. The basic equations are expressed in the partial differential form as,

Movement equation:

$$\frac{\partial Q}{\partial t}+\frac{\partial (Q^2/A)}{\partial x}+g\cos(i)A\frac{\partial h}{\partial x}=-g\frac{n^2 Q|Q|}{R^{4/3}A}+gA\sin(i) \qquad (1)$$

Continuity equation:

$$\frac{\partial A}{\partial t}+\frac{\partial Q}{\partial x}=q \qquad (2)$$

where:

t: time [T]; v: velocity [L/T]; R: hydraulic radius [L];
A: wetted cross section area [L2]; q: lateral inflow [L3/(T.L)];
x: distance measured along the channel [L];
g: acceleration due to gravity [L/T2]; i: channel slope [L/L];
n: the flow resistance coefficient (Manning's coefficient).

The numerical solution of the governing equations is executed through two basic steps. First, the partial differential equations are approximated by algebraic finite difference equations. Second, the Newton-Raphson method is then used to solve the non-linear algebraic equations. The double sweep method is applied to solve the system of linear simultaneous equations.

3. MODEL APPLICATION

The input data include 4 heavy storms that hit the region starting at 1h, 28th Aug. to 27th Sept. 1994 (Fig. 2); the geometric data of the river network and facilities; water level at boundaries; area of each field plot by elevation. The calibration was first carried out in order to estimate the acceptable value of roughness coefficient n. The model calibration agreed very well, as illustrated in Fig. 3.

In order to improve the present drainage capacity, the conceptual idea can be formulated based on gate combination. In this study, two main operational scenarios are examined:

Case 1- All regulators are open. The lower basins will receive more water from the upper ones.

Case 2- All regulators are close. Each of five drainage basins, namely Nhu Trac, Huu Bi, Coc Thanh, Vinh Tri and Co Dam, works independently.

Case 1. All gates open

The simulated results are presented in Figs. 4 to 7. The variation of discharges along the Sat River is shown in Fig. 4. This river hydrographs show that discharge is increased as water accumulates and flows downstream the river, varying from section to section, depending on the size and the altitude of the field plot as well. The Sat River, 38km long, is collecting drainage water for the Vinh Tri station with its pumping capacity of 30.7 m^3/s. As can be seen, the river discharge is much lower than the pumping capacity at some periods. Consequently, the suction water levels at the pumping stations are not high enough as required, then finally causes low efficiency of the pump. It can be said that the water conveyance capability of the drainage system is limited and drainage facilities are not fully operational. Similar situation can be observed at other rivers connecting to stations.

Figure 5 shows the flooding process at some selected field plots located at Vinh Tri basin, along the Sat riverbanks, which demonstrates the fluctuation of flooded water levels and flooded areas with respect to time. It shows that the water levels in the fields were increased and reached their maximum values on the 3rd and the day 20th after the flood came, and then gradually decreased as all of the pumping stations were being in operation.

By observing the flooding process hydrograph, we can easily locate the long-lasting period of flood at a certain submerged water depth as well as maximum water level at any field plot and how long the crops have remained submerged. Furthermore, together with information on kind, excess water-logging stress/tolerant of crops and so on, flood damage to crop production can be estimated. Similarly, flood damages to other economic activities can also be evaluated.

Case 2. All gates close

This alternative will divide the area into 5 polders separately. The advantage of this alternative is that drainage system of each polder can be operated independently so that less co-ordination in operation is required.

Figure 6 shows the comparison of computed water levels at some selected field plots in Vinh Tri basin for both cases, which shows about 0.2-0.3 m increased water level at peak. The same increment can be observed in Nhu Trac and Vinh Tri basins. However, in case of pumping stations having high capacities as in the case of Co Dam (42.8 m^3/s) and Coc Thanh (43.10 m^3/s), inundation can be reduced as seen in Fig. 7.

4. CONCLUSIONS

This paper presents the development of the model for flood control in pumped field lowland. The model is aimed at properly operating the drainage system by integrating series data such as GIS, river network, facilities, hydrology, weather data, etc. The simulated results show the flooding process at any field plot, at any location along the drainage channel, including water level, discharge, inundation area and submerged depth as well.

The study demonstrates two main operational scenarios based on gates operating condition. If all regulators are kept close, the pumping systems will work independently. In case of all regulators are open, the pumping systems should be co-operated. It is recommended that the former can be applied when heavy rain or evenly distributed rain falls in the area. The later can practically be utilized when rain falls unevenly distributed in the area. Besides, there are many ways of control system toward individual operation or system operation, depending on gates operated.

REFERENCES

1. Don, N.C. (1998). *Application of Interior Boundary Conditions in Unsteady Flow Computation.* AIT Thesis, WM 98-18, Asian Institute of Technology, Bangkok, Thailand.
2. Don N.C, Araki H., Yamanishi H. and Koga K. (2002). *Development of a Model for Flood Control in Namha, Vietnam.* Proceeding of International Association of Lowland Technology. Institute of Lowland Technology, Saga University.
3. Koga K., Araki H. and Baltasar F.J. van Dijk. (1994). *Water Environmental Management in Lowlands in Japan.* ILT 94 Seminar. Institute of Lowland Technology, Saga University.

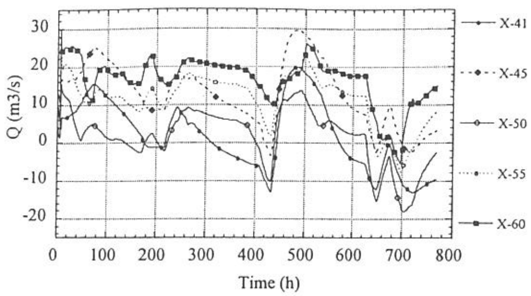

Fig. 4 Variation of Discharge along the Sat River

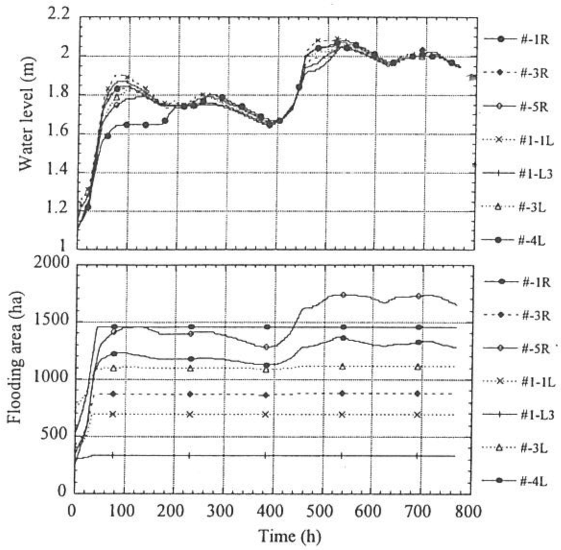

Fig. 5 Flooding process at field plots in Vinh Tri basin

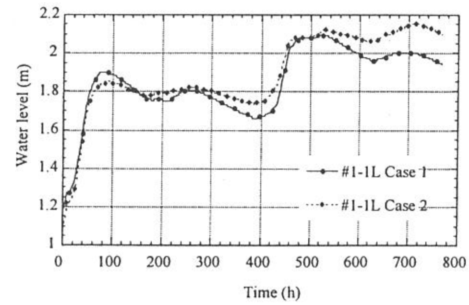

Fig. 6 Comparison of water level at field plot in Vinh Tri basin

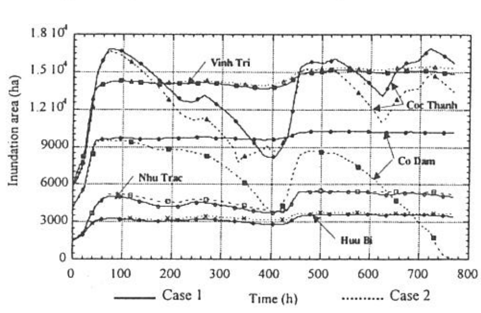

Fig. 7 Inundation area in sub-drainage basins